Model Prediction of the ESCR of Semicrystalline Polyethylene: Effects of Melt Cooling Rate

A. Sharif, N. Mohammadi, S. R. Ghaffarian

Loghman Fundamental Research Group, Polymer Engineering Department, Amirkabir University of Technology, Tehran, Iran

Received 26 July 2008; accepted 18 December 2008
DOI 10.1002/app.29893
Published online 26 February 2009 in Wiley InterScience (www.interscience.wiley.com).

ABSTRACT: The effects of melt cooling rate on the morphology and environmental stress cracking resistance (ESCR) of a commercial-grade high-density polyethylene (HDPE) were investigated by DSC, WAXS, Raman spectroscopy, DMTA, microhardness, and standard Bell test. The results showed exclusion of short chain branches from the crystallites leading to their perfection by decrease in the melt cooling rate. Accordingly, samples' ESCR increased because of the aforementioned crystal thickening. In addition, quantitative evaluation of crystal strength was performed for the first time by microhardness technique. Crystal strength or the required energy for plastic deformation of unit area of the crystals, $\Delta h \cdot \ell_c$, complemented crystal thickening hypothesis. The product of Δh and average crystal thickness, ℓ_c, was also proportional with storage modulus of the samples at ESCR test temperature. The evaluation of the results using the recently proposed model based on the analogy of crack growth through amorphous phase of semicrystalline polymers in harsh environments with crack growth at adhesive polymer–substrate interfaces showed reasonably good correlation. Finally, the comparison of literature and current research data based on the new model delineated new directions for phenomenon generalization. © 2009 Wiley Periodicals, Inc. J Appl Polym Sci 112: 3249–3256, 2009

Key words: polyethylene; environmental stress cracking resistance; crystal strength; model prediction

INTRODUCTION

Environmental stress cracking resistance (ESCR) of polyethylene (PE), the most consumed plastic, is of great importance from both academic and industrial points of view.[1–3] Slow crack growth (SCG) is the major process that controls PE failure under stresses far below its yield point in the presence of surface-active substances such as alcohols, soaps, and wetting agents.[4] Molecular weight, molecular weight distribution, comonomer type and content, chemical composition distribution, and environmental characteristics are the main parameters affecting SCG in PE. Accordingly, they were extensively investigated and elaborated in the literature.[5–11] Overlapping nature of the molecular parameters as well as their interplay with sample morphology often makes exact establishment of structure–property relationships difficult particularly regarding long-term character of the failure process.[12] Morphology of semicrystalline polymers depends on the conditions of thermal treatment and therefore can be altered in a broad range.[13–16] Nevertheless, few research works were devoted to the elucidation of thermal treatments role on the resistance of PE against slow crack growth (SCG) especially in the presence of a surface-active agent. Furthermore, the limited available data are often contradictory. For example, Runt and Jacq[17] investigated the influence of crystalline morphology on SCG rate of slightly branched PE in various samples with different thermal treatments. Larger spherulite size and size distribution appeared deleterious in the sample resistance against crack growth. In contrast, Yeh and Runt[18] reported no significant difference in SCG resistance of a high-density polyethylene (HDPE) prepared via different thermal treatments. Lu and Brown[19] also focused on the determination of cooling rate from the melt-state effects on the kinetics of SCG in a HDPE at 42°C. They found increase in the SCG rate by raising the cooling rate. The lower SCG rate of slowly cooled sample in comparison with rapidly cooled one was attributed to the higher yield point of the former at room temperature. They actually disregarded disentanglement rate of fibrils as an important controlling factor of the phenomenon, primarily affected by molecular weight and branch content. On the other hand, Strebel and Moet[12] reported completely different results regarding the thermal history effect on slow crack propagation in a medium-density PE during a fatigue test at room temperature. They explained their observations in terms of tie molecules,

Correspondence to: N. Mohammadi (mohamadi@aut.ac.ir).

connecting adjacent crystalline lamellae, and density. In other words, reduced crack propagation resistance of their slowly cooled material was ascribed to lower tie molecules concentration when compared with the quenched sample.

The effect of annealing for a finite time at various temperatures on the SCG of PE has been performed to illuminate the involved mechanisms. For example, Lu et al.[20] demonstrated maximum failure time for the treated sample at an intermediate annealing temperature between 86°C and its melting point. In fact, increase in the annealing temperature caused enhanced lamellae perfection leading to increased time to failure. Nevertheless, it also resulted in the decrease of tie molecules, which is in favor of the decrease in the failure time.

ESC prediction of various semicrystalline polymers seems an elusive goal with industrial importance, whose success is also a measure of scientific maturation of the field.[3,21] In an attempt to predict the SCG rate of PE, Huang and Brown[22] introduced a model by scaling approach-based characterization of tie molecules disentanglement rates as follows:

$$\delta_0 = A\lambda/(B\ \ell_c\, t)\sigma^n \exp(-Q/RT) \quad (1)$$

where δ_0, A, β, B, ℓ_c, t, σ, n, Q, R, and T are the rate of crack opening displacement, a constant, fraction of mobile tie molecules, a constant related to the anchoring strength of tie molecules in the crystals, crystal thickness, number of taut tie molecules per unit cross-section area of the fibril, applied stress, material parameter, activation energy for the micromolecular motion, gas constant, and test temperature, respectively. Quite recently, Sharif et al.[23] proposed a model based on the analogy of crack growth through amorphous phase of semicrystalline polymers in harsh environments with crack growth at adhesive polymer–substrate interfaces. They showed that time to failure, t_f, of various PEs with different weight-average molecular weights, M_w, and molecular weight distributions, PDI, correlated quite well through a sigmoidal-type equation with sample molecular characteristics. They are the area fraction of tie molecules at the crystal–amorphous interface (F_s), degree of amorphous phase mobility, quantified by the tan δ at β-transition, average crystal strength against stem sliding, estimated by the value of storage modulus at test temperature, E', and crack growth tortuosity parameter, Γ, estimated by M_w, PDI, is given as follows:

$$t_f = a[1 + \exp((b - G_c\Gamma)/c)]^{-1} \quad (2)$$

where $a = 3386$, $b = 0.16$, and $c = 0.006$ are equation constants. In addition, the term $E'F_s$ tan δ was assigned a measure of practical work of crack growth, G_c ($G_c = E'F_s$ tan δ).

The aim of this article is to study the sample cooling rate effects over the morphology and resultant ESCR of a commercial-grade HDPE and its possible consideration in the Sharif et al.'s model evaluation.

EXPERIMENTAL SECTION

Materials

The HDPE sample was a copolymer of ethylene with a small amount of propylene supplied by Bandar Imam Petrochemical Company of Iran (Poliran HB0035). The number-average and weight-average molecular weights as well as PDI were obtained by gel permeation chromatography (GPC). GPC data was collected using 1,2,4-trichlorobenzene as solvent at 150°C in a WATERS GPC2000 instrument. Polystyrene standards were used for universal calibration. Also, the branch content of the sample was obtained by Fourier transform infrared (Bruker Equinox 55 FTIR) spectroscopy. Characterization data along with the density of the sample at room temperature and melt index (MI) are given in Table I.

Sample Preparation

The pellets of the material were compression-molded into 2-mm-thick sheets after being melted for 10 min at 190°C in a hot press. Sheets of HDPE were then cooled down to room temperature with three procedures. Slowly cooled HDPE (SC-HD) was produced through the sheet's temperature drop to ambient in the press over 6 h. Controlled cooled sample (CC-HD), however, was prepared with a cooling rate at about 10°C/min via running cold water through the press platens. The quenched specimen (QU-HD) was obtained through cooling the melt sheet directly in an ice water bath.

Differential scanning calorimetry

The thermal properties of the samples were determined with a differential scanning calorimetry (DSC) instrument (TA 2010). Indium and tin were used for the calibration of the heat of fusion and melting temperature. Discs of about 7 mg were cut out of sample sheets heated in closed pans from room temperature to 160°C at 10°C/min, under nitrogen flux. Degree of crystallinity was calculated

TABLE I
Characteristics of the Studied HDPE

Sample	M_w	PDI	Branch content (CH_3/1000)	Density (g/cm^3)	MFI (g/10 min) (190°C at 2.16 kg)
HDPE	225,000	20.5	3	0.95	0.35

from the DSC traces using the enthalpy of fusion of the perfectly crystalline PE (293 J/cm^3).[24]

Raman Spectroscopy

Low-acoustic-frequency Raman spectra, in the range 5–60 cm^{-1}, were recorded on a Nicolet Almega Dispersive Raman spectrometer equipped with second harmonic frequency of a Nd : YLF laser operating at 532 nm. The power at the sample was 30 mW with the scattered light being collected at a 90° angle to the exciting beam. The frequency shift of a peak associated with the longitudinal acoustic mode (LAM) with respect to the frequency of the excitation light, $\Delta\nu$, expressed in cm^{-1}, depends on the length of the crystalline stem, ℓ, and on the velocity of sound along the chain in the following way[25]:

$$\Delta v = (1/2c\ell)(E/\rho_c)^{0.5} \quad (3)$$

where E, c, and ρ_c are Young's modulus of PE crystals in the direction of chain (290 GPa),[26] velocity of light, and the crystal density (1 g/cm^3),[27] respectively. Average thickness of crystalline lamellae, ℓ_c, was calculated from the crystalline stem length, ℓ, by correcting for a chain tilt of 30°.[26]

Wide-angle X-ray scattering

Wide-angle X-ray scattering (WAXS) of the samples was recorded in a transmission mode with Ni-filtered Cu Kα radiation ($\lambda = 0.154056$ nm) at a generator voltage of 30 kV and a generator current of 30 mA in a Philips Expert diffractometer. The WAXS raw data were collected between 12° and 28°, background-corrected and fitted by three Gaussian functions, representing the amorphous halo, and the 110 and 200 orthorhombic reflections. The intensity of the amorphous halo and two crystalline reflections were weighted and served for calculation of the degree of crystallinity.

Dynamic mechanical thermal analysis

Dynamic mechanical properties of different samples were probed in the bending mode with the dynamic mechanical thermal analyzer (DMTA) (Tritec, 2000 DMA) with a frequency of 1 Hz from −100 to 120°C at a heating rate of 2°C/min under nitrogen atmosphere.

Microindentation hardness

Microhardness of the samples was measured on a standard Vickers type instrument (Leica, VMHT) at room temperature (25°C). The indenter was a square-shaped diamond pyramid, with top angle of 136°. Loads of 0.2, 0.5, and 0.8 N were employed to correct the instant elastic recovery. A loading cycle of 0.1 min was used to minimize the creep effect. The microhardness (H) was determined by the following equation:

$$H = kP/d^2 \quad (4)$$

where P is the applied load, k is a geometric factor equal to 1.854, and d is the mean diagonal length of the imprint after removing indenter. At least 10 imprints were made under each load. The H value was determined within $\Delta H/H = 0.05$.

Environmental stress cracking resistance test

The ESCR was assessed according to the standard Bell-test (ASTM D 1693), which consisted clamping a notched rectangular piece, 38 × 13 × 1.9 mm^3 of material into bend position to activate stress cracking in the more strained region. Ten pieces of every material were tested simultaneously in a solution of 10 vol % Igepal Co-630 in distilled water at 50°C. Failure time (t_f) was defined as the time when 50% of the specimens displayed a visible crack at naked eye.

RESULTS AND DISCUSSION

The melting temperature and peak area or heat of fusion (ΔH_m) of the crystallized HDPE under different cooling rates, obtained from DSC measurements, are listed in Table II. The melting temperature is at 136°C for SC-HD and 134.5°C for CC-HD and QU-HD, respectively. The variation of melting temperature with respect to the thermal treatment is possibly due to the variation in crystal perfection. However, here, no difference could be detected between the melting temperature of the controlled-cooled and quenched samples. Simon et al.[15] also reported the same melting temperatures for controlled-cooled (10°C/min) and quenched (in ice-water bath) slightly branched PE samples. On the other hand,

TABLE II
Thermal Properties and Crystal Thicknesses of the Samples

Sample	T_m (°C)	ΔH_m (J/cm^3)	X (%)[a]	V_c (%)[b]	ℓ_c (nm)[c]
SC-HD	136	234	80	77	24.5
CC-HD	134.5	214	73	70	18.5
QU-HD	134.5	205	70	67	15.8

[a] Weight fraction of crystals.
[b] Volumetric percentage of crystallinity calculated from the relation, $V_c = X/(X+(100 - x)/\rho_a)$, where $\rho_a = 0.86$ g/cm^3 is the amorphous phase density of polyethylene.
[c] Crystal thickness calculated based on the LAM-Raman data.

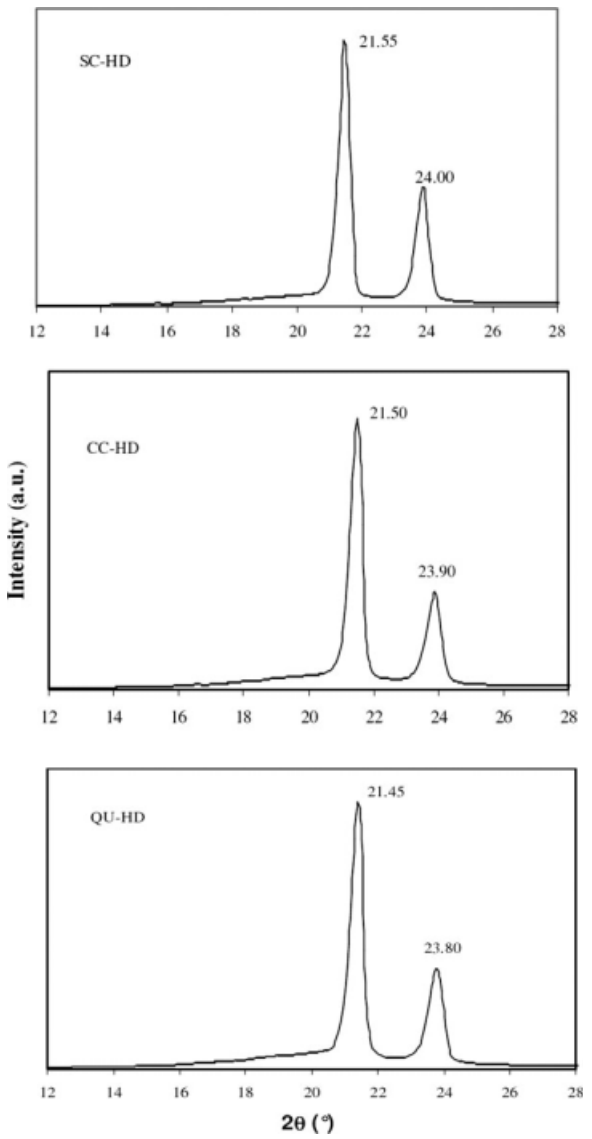

Figure 1 X-ray diffraction profiles of SC-HD, CC-HD, and QU-HD samples.

heat of fusion showed strong dependence on cooling rates. Higher cooling rate corresponded lower heat of fusion and thereby lower crystallinity (Table II). The crystalline growth would be expected to be mainly spherulitic consisting of well-organized lamellar structure due to preparation of the samples through different cooling procedures from the same HDPE melt.[28] For quenched samples, however, more folded chain lamellar structure may induce lower crystallinity, whereas a well-organized lamellar ridge-like structure may develop in the slowly cooled sample, leading to an average thickness of crystalline lamellae and crystallinity increase[29] (Table II).

The effects of cooling rate on the overall features of the WAXS diffractograms for the various PE samples are shown in Figure 1. Two reflections of the orthorhombic PE cell, the (110) and (200) planes are present in the WAXS patterns of the specimens from left to right. The peak reflections of the (110) and (200) planes of CC-HD and QU-HD are shifted to lower 2θ values when compared with the peaks of the SC-HD sample corresponding to an increase of the unit cell parameters in cross-chain directions.[30] It is usually assumed that the short-chain branches are not incorporated into the crystal lattice, which is certainly correct if the crystallization occurs at low cooling rates.[31] On the other hand, by rapid cooling or quenching of the samples, the primary crystallization occurs at larger supercooling and rates where the individual branches from the crystallites does not exclude completely.[31] Therefore, the aforementioned shifts of 2θ values are attributed to an increasing imperfection of crystals in samples with faster cooling. Accordingly, the degree of crystallinity derived from X-ray diffraction decreased with the increase in the cooling rate during melt crystallization (Table II). The crystallinity obtained by X-ray diffraction and DSC, however, were in close agreement, and their average value was used for further calculations.

The peaks corresponding to β- and α-relaxations in tan δ (T) curves for three specimens are shown in Figure 2. The cooling rate increase resulted in the decrease of α-relaxation temperature. On the other hand, the intensities and peak temperatures of the β-relaxations increased with the increase in the cooling rate during the crystallization process. The unexpected result of higher β-peak temperature of CC-HD in comparison with SC-HD can be rationalized with the exclusion of short-chain branches from the crystalline lattice of the latter. However, there existed no clear-cut maximum in the β-relaxation range of QU-HD sample. Apparently, β-peak of relaxation of

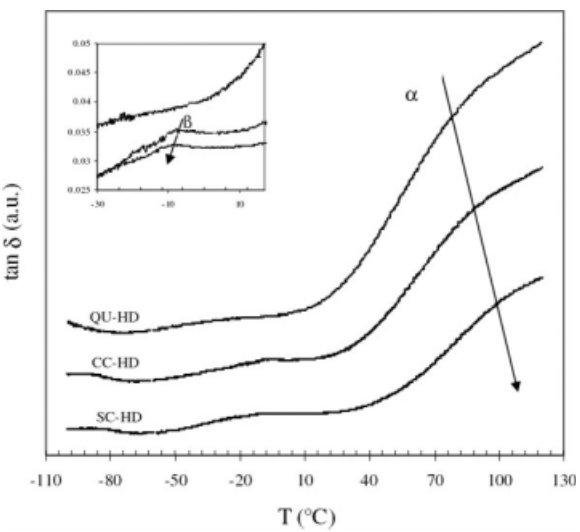

Figure 2 Tan δ behavior of various HDPEs. Inset figure shows the enlarged view of tan δ at β-relaxation region.

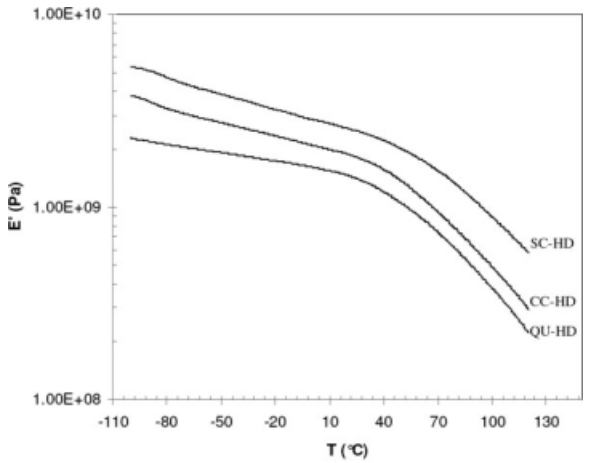

Figure 3 Temperature dependence of the storage modulus, E', of various HDPEs.

the QU-HD sample shifted so much toward its α-relaxation that overlapped with it. In fact, the extra loose amorphous phase of slowly cooled sample, due to major rejection of its short branches from the crystals and their more uniform distribution, lead to β-relaxation shift to lower temperature. Furthermore, facilitated cooperative segmental motion as a result of a reduction of specific crystal surface in slowly cooled sample may be considered as another explanation for this observation.[31]

Storage modulus, E', of the samples are shown in Figure 3. The increase in cooling rate reduced the storage modulus and elasticity of the sample. Storage modulus reduction can be directly attributed to the decrease in the sample crystallinity.[31]

Times to failure of the samples in the Bell-ESCR test are reported in Table III. Slowly cooled sample showed the highest ESCR in the Igepal solution while cooling rate increase reduced ESCR. Tie molecules concentration is one of the major controlling parameters in the ESCR of semicrystalline polymers.[21,32–34] In other words, greater tie molecules density leads to higher ESCR. Tie molecules' surface fraction at the crystal–amorphous interface (F_s) of the HDPE samples were calculated based on the equation recently suggested by Seguela[35]:

$$F_s = P\rho N_A l_0 s_0 / M_0(1 - V_c) \tag{5}$$

where P, ρ, N_A, l_0, s_0, M_0, and V_c are probability of forming a tie molecule per chain, polymer density, Avogadro's number, length of a monomer unit (0.25 nm for PE), the cross-sectional area of a single stem emerging from the crystal surface (0.18 nm^2 for PE), molecular weight of a monomer unit (28 g/mol for PE), and crystal volume fraction, respectively. P, the probability of intercrystalline tie molecules formation in a chain during its crystallization from the melt, is quantified by counting chain segments long enough to span an amorphous layer plus two adjacent crystalline lamellae[22]:

$$P = \frac{\int_L^\infty r^2 \exp(-b^2 r^2) dr}{3\int_0^\infty r^2 \exp(-b^2 r^2) dr} \tag{6}$$

where b^2 is equal to $3/2\langle h^2\rangle$ and $\langle h^2\rangle = C_\infty n l^2$ is the mean-square end-to-end distance of the entire chain in a random coil conformation.

In other words, chain segments longer than $L = 2\ell_c + \ell_a$ form tie molecules, where ℓ_c and ℓ_a are the thicknesses of crystal lamella and amorphous layer, respectively. For PE, $C_\infty = 6.8$, $l = 0.153$ nm, and n are the characteristic ratio, C—C bond length, and number of bonds, respectively. The value L in the lower limit of the integration in eq. (6) holds for the computation of the number of chain segments having an end-to-end distance greater than L. The factor 3 in the denominator of eq. (6) denotes the effect of lamella geometry that each tie molecule forms along one of its dimensions.

The L value can be calculated via eqs. (7) and (8)[36] as follows:

$$L = 2\ell_c + \ell_a \tag{7}$$

$$\ell_a = \ell_c(1 - X_c)/(0.86X_c) \tag{8}$$

According to the recent report by Men et al.,[37] the tan δ at β-relaxation is a measure of the amorphous phase mobility and would be directly related to the stress cracking resistance. They showed that failure time in full notch creep test (FNCT) increases exponentially with increasing amorphous phase mobility, represented by tan δ at −25°C. Nevertheless, both F_s and tan δ at β-relaxation of the present samples increased with the enhancement of cooling rate, Figure 4, while their ESCR decreased accordingly.

Few authors have pointed out the key role of crystal's strength as tie molecules anchoring sites, by controlling SCG rate of PE.[20,36,38] Nonetheless, more elaboration on defining an appropriate quantitative measure of crystal strength still seems to be required. To shed more light on this issue, microindentation hardness measurements were carried out to provide valuable information regarding the

TABLE III
Failure Times in ESCR and Microindentation Hardness Data of the Samples

Sample	Failure time (h)	H (MPa)	H_c (MPa)	Δh (J/cm^3)
SC-HD	30	75	97.4	5.12
CC-HD	15	60	85.7	4.96
QU-HD	9	52	77.6	4.1

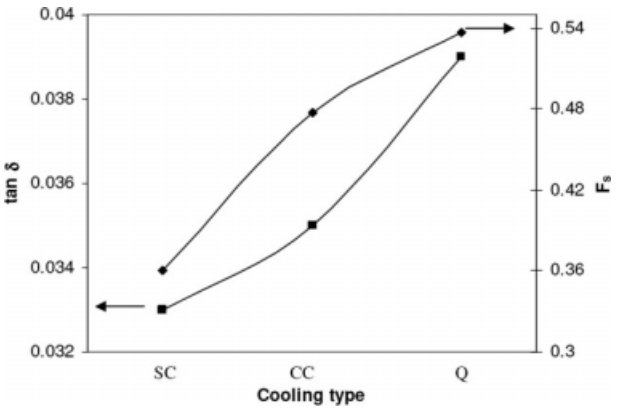

Figure 4 Variations of F_s and tan δ in the β-relaxation region of various HDPEs versus cooling type.

crystal strength.[39–41] The microindentation hardness, H (critical stress to deform a material mechanically) of semicrystalline polymers is related to the crystal hardness, H_c, through the following equation provided that plastic deformation takes place only in the crystalline region:

$$H = H_c V_c \tag{9}$$

where H_c itself is related to the average lamellar thickness through

$$H_c = H_c^{\infty}/[1 + (b/\ell_c)] \tag{10}$$

where $H_c^{\infty} = 170$ MPa is the hardness of an infinitely thick PE crystal and the mechanical parameter, $b = 2\sigma_e/\Delta h$ is the normalized folded surface free energy, σ_e, by the required energy for plastic deformation of unit volume of the crystals, Δh.[41] Accordingly, the quantity $\Delta h{\cdot}\ell_c$, in terms of energy per unit surface area (J/m^2), can be considered as the average resistance of crystalline lamellae against fragmentation and chain unfolding via dispatch of shearing planes. Δh values of the specimens were calculated by simultaneous application of eq. (10) and the Gibbs–Thomson relation [eq. (11)], Table III, as follows:

$$T_m = T_m^0[1 - (2\sigma_e/\rho_c \ell_c \Delta H_m^0)] \tag{11}$$

where T_m^0 and H_m^0 are equilibrium melting temperature (141.4°C) and fusion enthalpy of the perfect PE crystal (293 J/cm^3), respectively. Calculated $\Delta h{\cdot}\ell_c$ of the samples increased with cooling rate decrease due to crystalline lamella resistance enhancement against fragmentation and chain unfolding leading to failure time increase, Figure 5. By including the contribution of crystal strength on SCG rate, different ESCRs of three thermally treated HDPE samples can now be rationalized.

A closer look at the SCG phenomenon delineates that it arises from the sporadic nucleation of cavities in the amorphous phase constrained between neighboring crystalline lamella.[4,42] Then, localized plastic yielding occurs in the proximity of the cavities, accompanied with fragmentation of the crystalline lamellae and their partial chain unfolding. The initial damage gradually grows into a craze, i.e., a crack bridged by numerous microfibrils that prevent crack opening. A crack slowly develops from the craze under stress via rupturing of microfibrils and propagates through the bulk till the material failure.[4] Measurements of stress field on the craze boundary in PE by Wang and Brown[43] showed a maximum stress approximately equal to the material yield stress. This stress is too low to cause appreciable chain scission during microfibrils failure, and thus it may be expected to take place mainly through tie molecules pulling out the lamellae. Clearly, the strength of the anchoring tie molecules crystals, quantified by $\Delta h{\cdot}\ell_c$, plays an extremely important role both in nucleation and propagation stages of slow crack process. Therefore, the results of this research work suggested that the exclusion of short-chain branches from the crystalline region, for example, SC-HD sample, led to the increase in the time to failure because of the more perfect crystalline lamellae formation and disentanglement rate of tie molecules decrease.

All the aforementioned key parameters in the ESCR of semicrystalline polymers were included in Sharif et al.'s model.[23] The strength of lamellae against stem sliding, however, was estimated by the sample's storage modulus at test temperature. Storage modulus or sample elasticity at test temperature, 50°C, is another measure of the crystalline lamellae strength against fragmentation and unfolding.[44] In other words, E' is proportional with $\Delta h{\cdot}\ell_c$ and therefore they can be used interchangeably, Figure 5. The calculated values of E', F_s, tan δ, and Γ of the

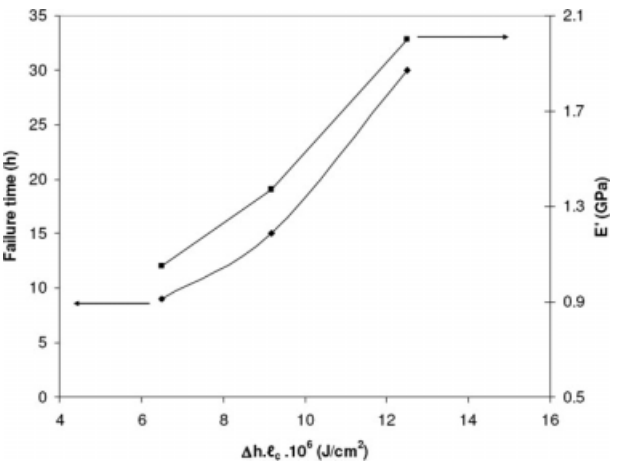

Figure 5 Variations of failure time and storage modulus at 50°C versus $\Delta h{\cdot}\ell_c$ of various HDPEs.

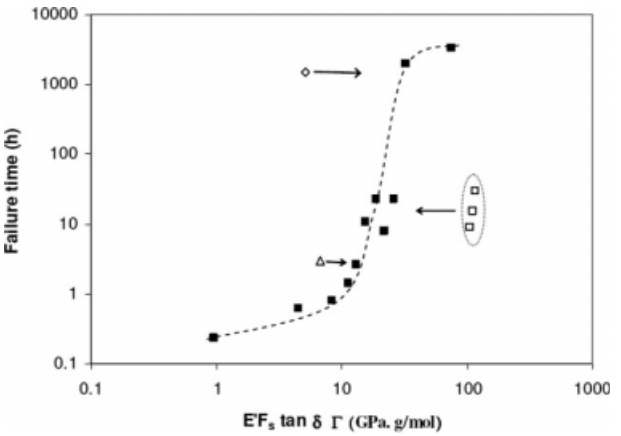

Figure 6 Failure times of the samples as a function of E', F_s, tan δ, Γ for the present HDPE (□), LLDPE (◊), LDPE (△), and Men et al.[37] (■) samples.

studied samples exhibited a good log–log correlation to their time to failure, t_f, measured by the standard Bell-test, Figure 6. For comparing the results of this research with Men et al.'s,[37] their data points were also included in the figure. In addition, measured time to failure of a low-density polyethylene (LDPE) and a linear low-density polyethylene (LLDPE), from this study, were also added to strengthen the following discussion and highlight other requirements for generalizing the model. The sigmoidal-type equation fitting on Men et al.'s[37] results based on newly proposed model[23] may contribute in the aforementioned direction. Data points of this research on time to failure of HDPEs, LDPE, and LLDPE samples stayed far away from those of Men et al.'s, but at right and left hand sides for the former and latter, respectively, Figure 6. Two major parameters, i.e., test configuration and stress intensity factor may contribute to the observed discrepancies. In other words, Men et al.[37] employed FNCT, which is a constant-stress method to evaluate the ESCR of their samples, whereas constant-strain Bell-test procedure was used in this research. In addition, even in a certain test method, stress intensity effect may lead to different responses among various samples. Lower crystallinities of the LLDPE (36%) and LDPE (31%) in comparison with the HDPEs might cause the original sharp notch to become blunter in the order of LDPE > LLDPE > HDPE.[36] Including the extent of blunting in the model probably modifies failure times in a way they may fit on another sigmoidal-type curve.

CONCLUSIONS

The cooling rate increase from the melt state was shown to decrease the time to failure of a commercial-grade HDPE in a Bell-ESCR test. The concepts of tie molecules concentration and amorphous phase mobility were verified to be not sufficient for describing the observed material behavior. Times to failure of the samples were shown to increase proportionally with crystals' strength enhancement quantified by $\Delta h \cdot \ell_c$ or their storage modulus at test temperature. The recently proposed model by Sharif et al., based on the analogy of crack growth through amorphous phase of semicrystalline polymers in a harsh environment with crack growth at adhesive polymer–substrate interfaces, predicted the samples' time to failure reasonably well.

References

1. Lagaron, J. M.; Dixon, M.; Gerrard, D.; Reed, W.; Kip, B. J. Macromolecules 1998, 31, 5845.
2. Munaro, M.; Akcelrud, L. Polym Degrad Stab 2008, 93, 43.
3. Soares, J. B. P.; Abbot, R. F.; Kim, J. D. J Polym Sci Part B: Polym Phys 2000, 38, 1267.
4. Cazenave, J.; Seguela, R.; Sixou, B.; Germain, Y. Polymer 2006, 47, 3904.
5. Huang, Y.; Brown, N. J Mater Sci 1988, 23, 3648.
6. Lu, X.; Ishikawa, N.; Brown, N. J Polym Sci Part B: Polym Phys 1996, 34, 1809.
7. Boehm, L. L.; Enderle, H. F.; Fleissner, M. Adv Mater 1992, 4, 231.
8. Huang, Y.; Brown, N. J Polym Sci Part B: Polym Phys 1990, 28, 2007.
9. Yeh, J. T.; Chen, C. Y.; Hong, H. S. J Appl Polym Sci 1994, 54, 2171.
10. Lagaron, J. M.; Pastor, J. M.; Kip, B. J. Polymer 1999, 40, 1629.
11. Ghanbari-Siahkali, A.; Kingshott, P.; Breiby, D. W.; Arleth, L.; Kjeellander, C. K.; Almadal, K. Polym Degrad Stab 2005, 89, 442.
12. Strebel, J. J.; Moet, A. J Polym Sci Part B: Polym Phys 1995, 33, 1969.
13. Peeters, M.; Goderis, B.; Vonk, C.; Reynaers, H.; Mathot, V. J Polym Sci Part B: Polym Phys 1997, 35, 2689.
14. Androcsh, R.; Wunderlich, B. Macromolecules 1999, 32, 7238.
15. Simon, L. C.; de Souz, R. F.; Soares, J. B. P.; Mauler, R. S. Polymer 2001, 42, 4885.
16. Minick, J.; Moet, A.; Baer, E. Polymer 1995, 36, 1923.
17. Runt, J.; Jacq, M. J Mater Sci 1989, 24, 1421.
18. Yeh, J. T.; Runt, J. J Polym Sci Part B: Polym Phys 1991, 26, 792.
19. Lu, X.; Brown, N. Polymer 1987, 28, 1505.
20. Lu, X.; McGhie, A.; Brown, N. J Polym Sci Part B: Polym Phys 1992, 30, 1207.
21. Ward, I. M.; Lu, X.; Huang, Y.; Brown, N. Polymer 1991, 32, 2172.
22. Huang, Y. L.; Brown, N. J Polym Sci Part B: Polym Phys 1991, 29, 129.
23. Sharif, A.; Mohammadi, N.; Ghaffarian, S. R. J Appl Polym Sci 2008, 110, 2756.
24. Wunderlich, B.; Czornyj, G. Macromolecules 1977, 10, 906.
25. Glotin, M.; Mandelkern, L. J Polym Sci Part B: Polym Let 1983, 21, 807.
26. Lu, L.; Alamo, R. G.; Mandelkern, L. Macromolecules 1994, 27, 6571.
27. Wunderlich, B.Macromolecular Physics Crystal Structure, Morphology, Defects; Academic Press: New York, 1973; Vol. 1.
28. Basset, D. C.Principles of Polymer Morphology; Cambridge University Press: London, 1981.

29. Kundu, P. P.; Biswas, J.; Kim, H.; Chung, C. W.; Choe, S. J Appl Polym Sci 2004, 91, 1427.
30. Simanke, A. G.; Alamo, R. G.; Galland, G. B.; Mauler, R. S. Macromolecules 2001, 34, 6959.
31. Kolesov, I. S.; Androsch, R.; Radusch, H. J. Macromolecules 2005, 38, 445.
32. Lustiger, A.; Corneliusen, R. D. J Mater Sci 1987, 22, 2470.
33. Schellenberg, J.; Fienhold, G. Polym Eng Sci 1998, 38, 1413.
34. Zhou, Z.; Brown, N. Polymer 1994, 35, 3619.
35. Seguela, R. J Polym Sci Part B: Polym Phys 2005, 43, 1729.
36. Brown, N.; Zhou, Z. Macromolecules 1995, 28, 1807.
37. Men, Y. F.; Rieger, J.; Enderle, H. F.; Lilge, D. Eur Phys J E 2004, 15, 421.
38. Brown, N.; Lu, X. Polymer 1995, 36, 543.
39. Balta Calleja, F. J. Trends Polym Sci 1994, 2, 419.
40. Flores, A.; Pietkiewicz, D.; Stribeck, N.; Roslaniec, Z.; Balta Calleja, F. J. Macromolecules 2001, 34, 8094.
41. Flores, A.; Mathot, V. B. F.; Michler, G. H.; Adhikari, R.; Balta Calleja, F. J. Polymer 2006, 47, 5602.
42. Plummer, C. J. G. Adv Polym Sci 2004, 169, 75.
43. Wang, X.; Brown, N. Polymer 1989, 30, 1456.
44. Boyd, R. H. Polymer 1985, 26, 1123.